International Journal of Materials Science and Applications
2025, Vol. 14, No. 4, pp. 134-143
https://doi.org/10.11648/j.ijmsa.20251404.13

Research Article

Study of the Effect of Interface Defect Layers (IDL_1 and IDL_2) on $CsGeI_3$ Perovskite Solar Cells by SCAPS 1D Simulation

Alioune Sow*, Saliou Seck, Modou Faye, Mamadou Salif Mane, Amadou Ndiaye, Bachirou Ndiaye, Babacar Mbow, Cheikh Sene

Department Physics, Faculty of Sciences and Technology, Semiconductors and Solar Energy Laboratory, Cheikh Anta DIOP University, Dakar, Senegal

Abstract

Germanium-based perovskite solar cells have garnered significant interest within the scientific community due to their non-toxicity and excellent stability. However, their low conversion efficiency is an obstacle to their application and design. We designed a device with a normal configuration structured as *Glass / FTO / SnO_2 / IDL_1 / $CsGeI_3$ / IDL_2 / Cu_2O / Au* to improve our germanium-based perovskite solar cell, designed The integration of interface defect layers IDL_1 and IDL_2 the reduction of recombination. The study revealed that these IDL_1 and IDL_2 layers play a crucial role in solar conversion performance. By adjusting the thickness, electron affinity and defect density of the IDL_1 and IDL_2 layers, the conversion efficiency of our device exceeds 19%. However, an increase in temperature in the environment can negatively affect the cell by decreasing its photovoltaic efficiency.

Keywords

Perovskite, $CsGeI_3$, IDL_1, IDL_2, *PCE* Performance

1. Introduction

In a global context where societaleVolution and the increasing energy demands of populations lead to a growing consumption rate of around 2.4% in 2023, this results in a significant rise in global pollution due to carbon dioxide (CO_2) emissions. According to estimates compiled by the global budget project, pollution will increase by 0.8% in 2024, or 37.4 billion metric tons, compared with 2023 [21]. The increase in global pollution is the main cause of climate change.

In order to neutralize carbon in industrial production, clean and efficient renewable energies are gaining popularity. The development of clean and sustainable energy sources has attracted attention over this century [1, 3, 20]. Solar energy has received considerable attention as a clean and non-polluting energy source with significant potential. In recent years, scientists have shown increasing interest in perovskite solar cells due to their remarkable light absorption capacity and promising prospects [4, 8, 12]. Currently, lead-based perovskite solar cell technology is being developed for commercialization, aiming to replace silicon solar cells [6, 19]. However, despite the vast application prospects of these perovskite solar cells, the toxicity and water solubility of lead are causing growing concern. In the field of lead-free perovskite solar cells, those based on germanium, due to their

*Corresponding author: Alioune902@gmail.com (Alioune Sow)

Received: 3 July 2025; **Accepted:** 16 July 2025; **Published:** 31 July 2025

low toxicity, represent a highly favorable option compared to lead-based ones [2, 14, 17]. Germanium-based perovskite offers the advantages of low toxicity to the environment and organisms, great stability, and a tunable bandgap [15]. Nevertheless, further research is needed to explore the extended application of germanium-based perovskite cells due to their low conversion performance compared to their lead-based counterparts.

In this work, we will use the SCAPS 1D software, a simulator, to contribute to improving the conversion yields of germanium-based perovskite solar cells, while also addressing potential issues in the design of the solar device. Thus, our study device will be under the normal n-i-p configuration structured as $Glass / FTO / SnO_2 / IDL_1 / CsGeI_3 / IDL_2 / Cu_2O / Au$. We have chosen SnO_2 and Cu_2O [1, 11, 18] as electron transport material (ETM) and hole transport material (HTM), respectively. Considering recombination and interface quality, we added defect interface layers (IDL_1 , IDL_2) [3, 7] on both sides of the perovskite layer. The objective is toeValuate the impact of defect interface layers on the performance of the designed device.

2. Parameters and Methodology

This work was conducted using the SCAPS 1D modeling software developed by the University of Ghent. This simulator primarily relies on solving three fundamental equations, which are Poisson's equation and the continuity equations [1, 16].

$$\frac{d}{dt}\left(\varepsilon(x)\frac{d\psi}{dx}\right)=q\left[p(x)-n(x)+N_D^+(x)-N_A^-(x)+p_t(x)-n_t(x)\right] \quad (1)$$

$$\nabla\overrightarrow{J_n}=q\left[R_n-G_n+\frac{\partial n}{\partial t}\right] \quad (2)$$

$$\nabla\overrightarrow{J_p}=q\left[R_p-G_p+\frac{\partial p}{\partial t}\right] \quad (3)$$

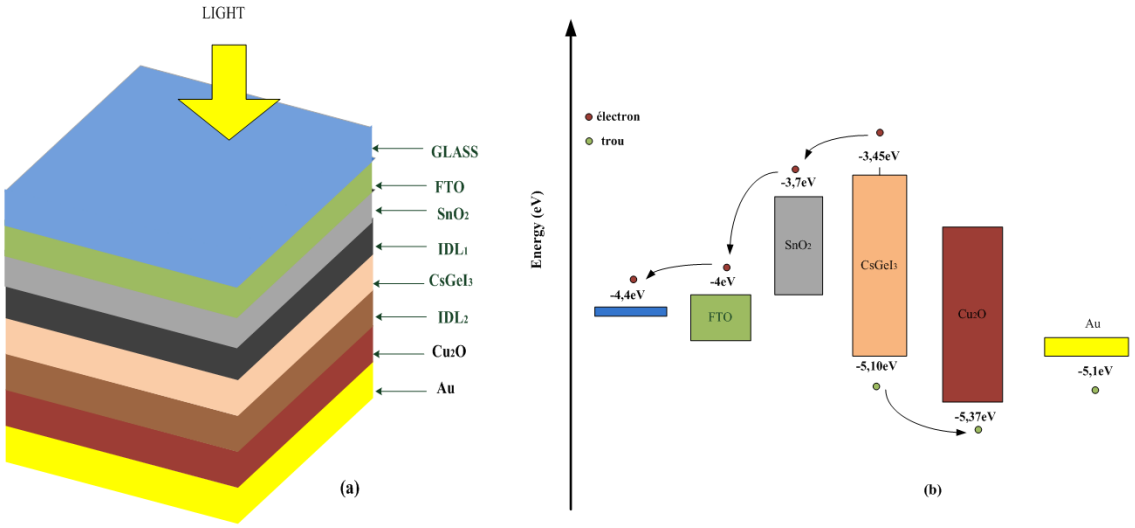

Figure 1. *Structure of the cell (a) and energy diagram (b).*

N is the concentration of free electrons and p is the concentration of free holes; n_t and p_t: represent the distribution of trapped electrons and holes respectively; N_D^+, N_A^-: ionized donor and acceptor doping concentrations, respectively.

Solving these equations allows us to obtain the modeling parameters [1]. Before that, it is imperative to define the structuring of our device. The figure below illustrates the arrangement of the various structural layers of the cell and the energy band diagram. We added IDL_1 and IDL_2 between the ETL and the perovskite layer and between the perovskite layer and the HTL, to prevent interface recombination and make the bandgap structure more resistant.

The values used for each layer for the simulation are listed in Table 1. In the table below, N_C and N_V correspond to the effective densities of the conduction band and the valence band, N_A and N_D denote the density of acceptor and donor respectively, μ_p and μ_n represent the mobility of holes and electrons respectively, χ represents the electron affinity, E_g is the bandgap energy, and ε_r is the relative permittivity. It can be noted that parameters for the metal layers ($Glass$ and Au) have been provided as they are taken as work functions with energy values of -4.4eV for $Glass$ [3, 10] and -5.1eV for Au [3, 7].

Table 1. *Parameters of the layers used.*

	FTO [3, 5, 10]	SnO_2 [1, 18]	IDL_1 [3, 5, 22]	$CsGeI_3$ [5, 13]	IDL_2 [3, 5, 22]	Cu_2O [1, 11, 18]
Eg (eV)	3.5	3.5	1.41	1.6	1.41	2.17
X (eV)	4.0	4.0	4.17	4.0	4.17	3.2
ε_r	9.0	9.0	8.2	18	8.2	7.1
$\mu_p(cm^2.V^-.s^{-1})$	10	10	1.6	20	1.6	80
$\mu_n(cm^2.V^-.s^{-1})$	20	20	1.6	20	1.6	2000
$N_V(cm^{-3})$	1.810^{19}	2.610^{21}	1.10^{18}	1.10^{19}	1.10^{18}	1.10^{18}
$N_C(cm^{-3})$	2.210^{18}	4.3610^{18}	1.10^{18}	1.10^{18}	1.10^{18}	2.210^{18}
$N_A(cm^{-3})$	0	0	1.10^{12}	2.10^{18}	1.10^{12}	1.10^{18}
$N_D(cm^{-3})$	2.10^{19}	1.10^{18}	0	2.10^{16}	0	0
$N_t(cm^{-3})$	1.10^{15}	1.10^{15}	1.10^{18}	1.10^{15}	1.10^{18}	1.10^{15}
Thickness (nm)	500	30	8	1000	8	1000

3. Results and Discussion

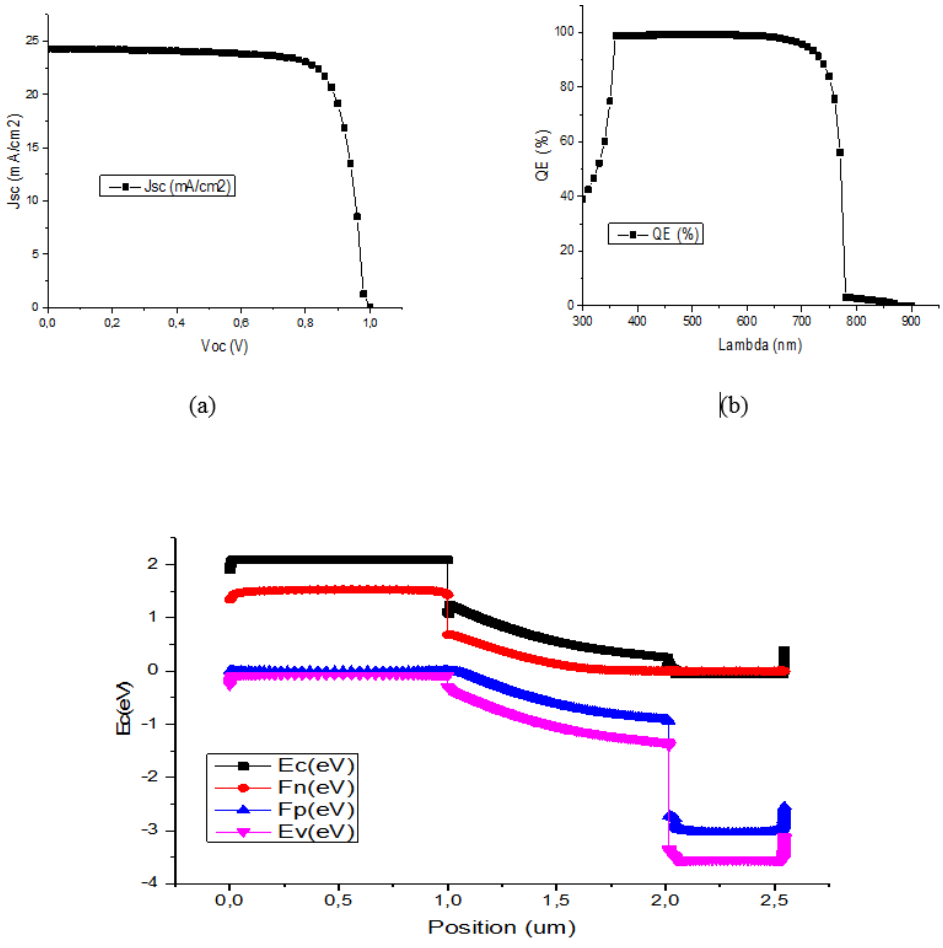

Figure 2. *Current density as a function of voltage (a), external quantum efficiency (b), and energy band diagram (c).*

With the data specified in the above table, we simulated using SCAPS 1D, allowing us to plot graphs of current density, external quantum efficiency, and energy bands. Figure 2a represents the relationship between current density J and open circuit voltage V_{OC}, showing a decrease in density as voltage increases. The modeling provided a voltage value (V_{OC}) of 0.98 V, a current density of 24.30 mA/cm², a fill factor of 78.67%, and finally a conversion efficiency from 18.79%. Figure 2b illustrates the external quantum efficiency, consisting of three parts: between 300 and 400nm indicating a growth phase of yield, from 400 to 700nm representing the highest phase of quantum yield, above 80%, and beyond 700nm, we note a drastic drop in the external quantum yield of our device. Figure 2c represents the energy bands, where E_c illustrates the conduction band energy level, F_n the Fermi level of electrons, F_p that of holes, and E_v the valence band. This graph shows that the gap between the conduction band level and the valence band level results in an electric field of approximately 2.11 V/µm. The conversion efficiency of the cell model can be improved by reducing recombination between the different layers. Therefore, we examine the impact of varying the parameters of the IDL layers on the performance of the solar cells.

3.1. Contribution of the Variation of the Thickness of the Interface Defect Layer on the Performances

To reduce recombination in our work cell, we added defect interface layers (IDL_1) between the electron transport layer (ETL) and the absorbing layer and (IDL_2) between the hole transport layer (HTL) and the $CsGeI_3$ layer. Given the significant impact of layer thickness on internal efficiency and carrier transport in perovskite-based solar cells, we felt it necessary to assess the contribution of varying layer IDL thicknesses on the efficiency of our cell. We fixed a thickness range for IDL_1 varying between 0.001 to 0.01µm and for layer IDL_2 between 0.001 to 0.004µm. The simulation with these values allowed us to plot the trends of the electrical parameters. Figure 3a shows that increasing the thickness of layer IDL_2 results in a slight drop in voltage, whereas the drastic decrease in open circuit voltage is more noticeable with the increase in thickness of layer IDL_1, dropping from 5.95 to 4.03V. This leads to a drop in the open-circuit voltage, if we take the difference between the two values indicated above, and it remains within the range of the band gap of our cell absorber. Therefore, the thickness of layer IDL_1 plays a major role in the open circuit voltage. Figure 3b represents current density as a function of IDL thickness variation. We see that increasing the thickness of layer IDL_1 does not significantly influence the current density. Conversely, increasing the thickness of layer IDL_2 leads to an increase in current density from 24.26mA/cm² for an IDL_2 thickness of 0.001µm to 24.29mA/cm² for an IDL_2 value of 0.004µm. Therefore, layer IDL_2 has a dominant influence on current density. Figure 3c shows the increase in fill factor as a function of increasing IDL layer thickness. A sufficient proof that the variation of the fill factor depends on theeVolution of the thicknesses of the IDL layers. Figure 3d illustrates the conversion efficiency diagram of our device, where we can see that the PCE under goes a slight decrease in its value with the increase in thickness of IDL_1. Conversely, the drop in yield is accentuated with theeVolution of thickness of IDL_2, which decreases its value from 19.06 to 18.87%. In summary, we can expect to achieve a better conversion efficiency of our device with thicknesses for the defect interface layers (IDL_1 and IDL_2) of 0.001µm.

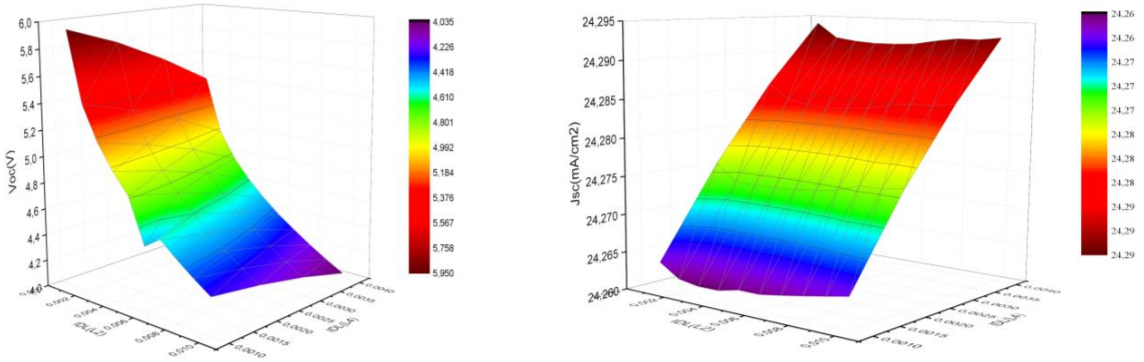

(a) (b)

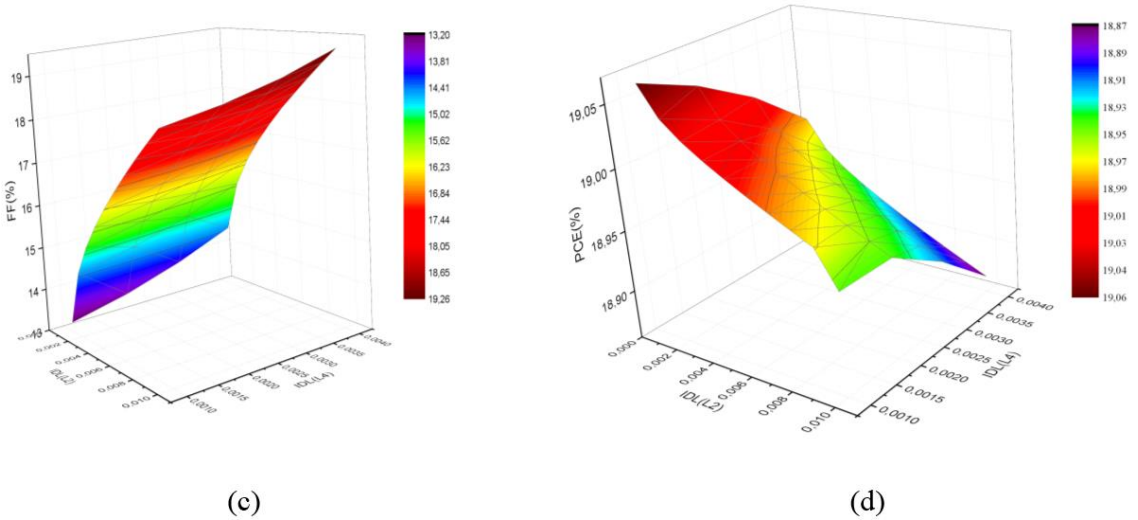

(c) (d)

Figure 3. *Effect of varying the thickness of interface defect layers: (a)* V_{OC} *, (b)* J_{SC} *, (c)* FF *, and (d)* PCE *.*

3.2. Impact of Electron Affinity on the Interface Defect Layers and on Performance

The electron affinity energy, which signifies the energy associated with the attraction of electrons, helps understand an element's likelihood of acquiring electrons. A level of electron affinity can enhance the performance of a solar cell. To better observe these effects, we have shown in Figure 4 the impact of varying the electron affinity energy of the interface layers. The energies of layers IDL_1 and IDL_2 were varied between a range of 4.12 and 4.17eV. Figure 4a shows that the variation of electron affinity in layer IDL_1 does not impact the open circuit voltage. However, increasing the electron affinity energy of layer IDL_2 causes a rapideVolution of V_{OC}. Therefore, the electron affinity level is more balanced in layer IDL_2, which explains its dominant impact compared to layer IDL_1. Figure 4b shows the current density according to the variation of electron affinity. We can see that the increase in electronic energy in layer IDL_1 leads to a drop in J_{sc} from almost 24.10 mA/cm ² to 24.00 mA/cm ². However, for layer IDL_2, increasing its electron affinity results in an increase in current density. The effect is therefore more significant in layer IDL_2. In the simulation, the best cell current density value is obtained with the layer and the layer for electron energy values of 4.12eV and 4.17eV respectively.

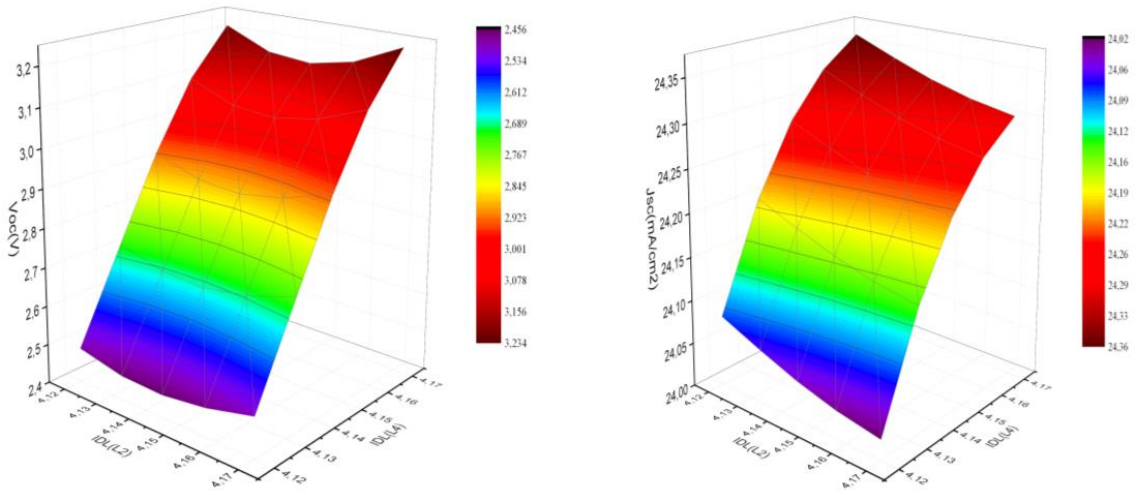

(a) (b)

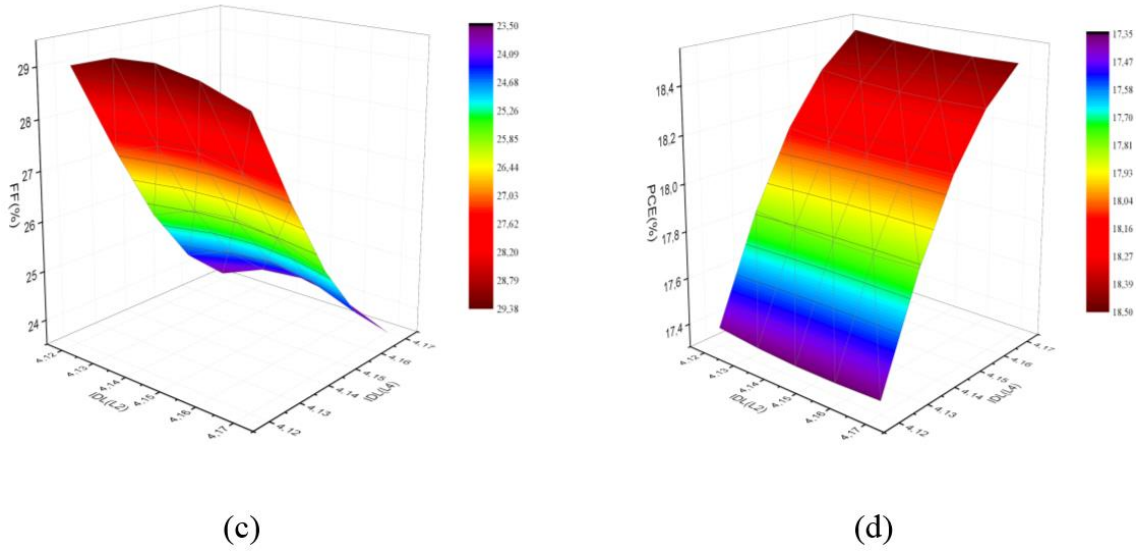

Figure 4. *Impact of varying electron affinity of interface defect layers: (a)* V_{OC} *, (b)* J_{SC} *, (c) FF, and (d)* PCE *.*

Regarding the fill factor (Figure 4c), its value remains constant regardless of the increase in electron affinity in layer IDL_1. Conversely, the variation of the fill factor is more pronounced as a function of theeVolution of electron affinity in layer IDL_2. We have seen a drastic reduction in the fill factor value from 29% for an affinity of 4.12eV to less than 24% with an affinity of 4.17eV for layer IDL_2. Figure 4d shows that increasing electron affinity in layer IDL_1 does not have major consequences, allowing the consistency of the conversion yield of our cell to be maintained. The increase in conversion performance is simply due to the addition of electron affinity in layer IDL_2. Therefore, increasing the electron affinity in layer IDL_2, which makes the system more stable and reduces electronic transitions. Consequently, a balanced electron affinity level in layer IDL_2, equivalent to 4.17eV, improves the cell efficiency to 18.50%.

3.3. Impact of Variation IDL Defect Density on Performance

In the field of semiconductor solar cells, effective management of defects plays a crucial role in influencing photovoltaic conversion efficiency. In addition to the thickness of the layer, the presence of defects on the layers also affects the cell's performance. To conduct a thorough analysis, we represented the effect of varying the defect density between 10^{15} and $10^{18}\ cm^{-3}$ in the IDL layers on the electrical parameters in the figure below. Figure 5a shows that the variation of defect density in layer IDL_1 does not have much impact on the open circuit voltage. However, increasing defects in layer IDL_2 causes a drop in the open circuit voltage V_{OC}. On the layer, for a defect rate of $10^{18} cm^{-3}$, we can see that the is at its smallest value. In Figure 5b, the decrease in current density is most noticeable when the defect rate present in the layer is between 10^{15} and $10^{17} cm^{-3}$. Beyond this value, the presence of a fault IDL_1 in the layer has no effect on the current density. Regarding layer IDL_2, increasing the defect density leads to a decrease in current density in this layer. The effect of defects is more pronounced in layer IDL_2 than in layer IDL_1. In Figure 5c, the fill factor is not significantly influenced by the increase in defect density in layer IDL_1. Although there is a slight variation in the fill factor in graph 5.c, it is too small to be significant. We can see from this graph that the decrease in the cell's conversion efficiency is systematically linked to the existence of defects IDL in the layers. The conversion efficiency of the cell decreases from 19.01% for a defect rate of $10^{15} cm^{-3}$ to 18.47% when the defect rate present is $10^{18}\ cm^{-3}$. Figure 5d shows the variation of the conversion efficiency of our cell as a function of the increase in defects in the interface layers. We can see that the decrease in conversion efficiency of the cell is systematically linked to the injection of defects in the IDL layers. The conversion efficiency thus drops from 19.01% for defects of $10^{15}\ cm^{-3}$ to 18.47% for defects of $10^{18}\ cm^{-3}$. In summary, the analysis of Figure 5d reveals that the increase in defect density hampers the efficiency of carrier flow. It increases the probability of recombination of electron-hole pairs, especially in the layer IDL_2, and consequently reduces the performance of the device.

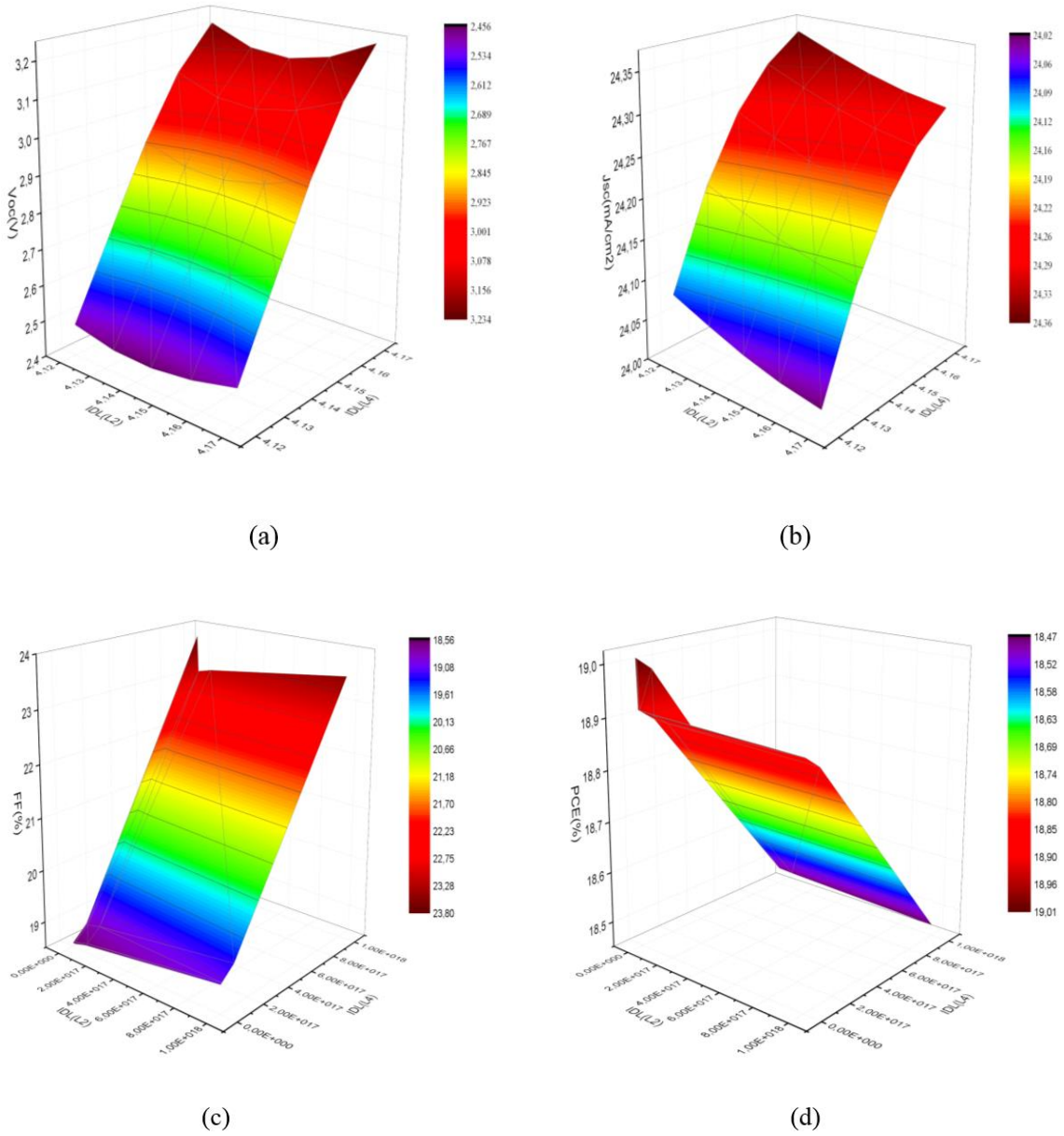

Figure 5. *Impact of variation defect density of interface defect layers: (a)* V_{OC} *, (b)* J_{SC} *, (c)* FF *, and (d)* PCE *.*

3.4. Effect of Operating Temperature on Photovoltaic Performance

One of the factors that greatly influences the performance and stability of perovskite-based solar cells is temperature [9]. To study its effect on our device, we adjusted the temperature between 300 ℃ and 600 ℃ and observed its behavior on the J-V characteristics as well as on the electrical parameters. In Figure 6a, we find that the J-V characteristics of the cell weaken with the increase in temperature. This shows that the J-V characteristic is strongly influenced by temperature. The decrease in cell characteristics with the increase in temperature may be caused by the degradation of the perovskite cell crystal. In Figure 6b to 6e, we represented the electrical parameters extracted from the J-V characteristic curve. In Figure 6b, the increase in temperature causes a decrease in open circuit voltage, indicating that temperature affects the series resistances of the device. Figure 6c shows that the impact of temperature on current density is almost negligible, resulting in a constant value of J_{SC} whatever the temperature used. Regarding the fill factor illustrated by Figure 6d, we note an increase in the fill factor between 300 ℃ and 400 ℃, reaching its best value at 400 ℃, close to 80%. Beyond 400 ℃, the increase in temperature leads to a decrease in fill factor. In Figure 6e, we clearly observe that temperature has a negative effect on the efficiency of the solar cell's performance, which is explained by the fact that high temperatures lead to the destruction and volatility of certain components, as well as instability in the device.

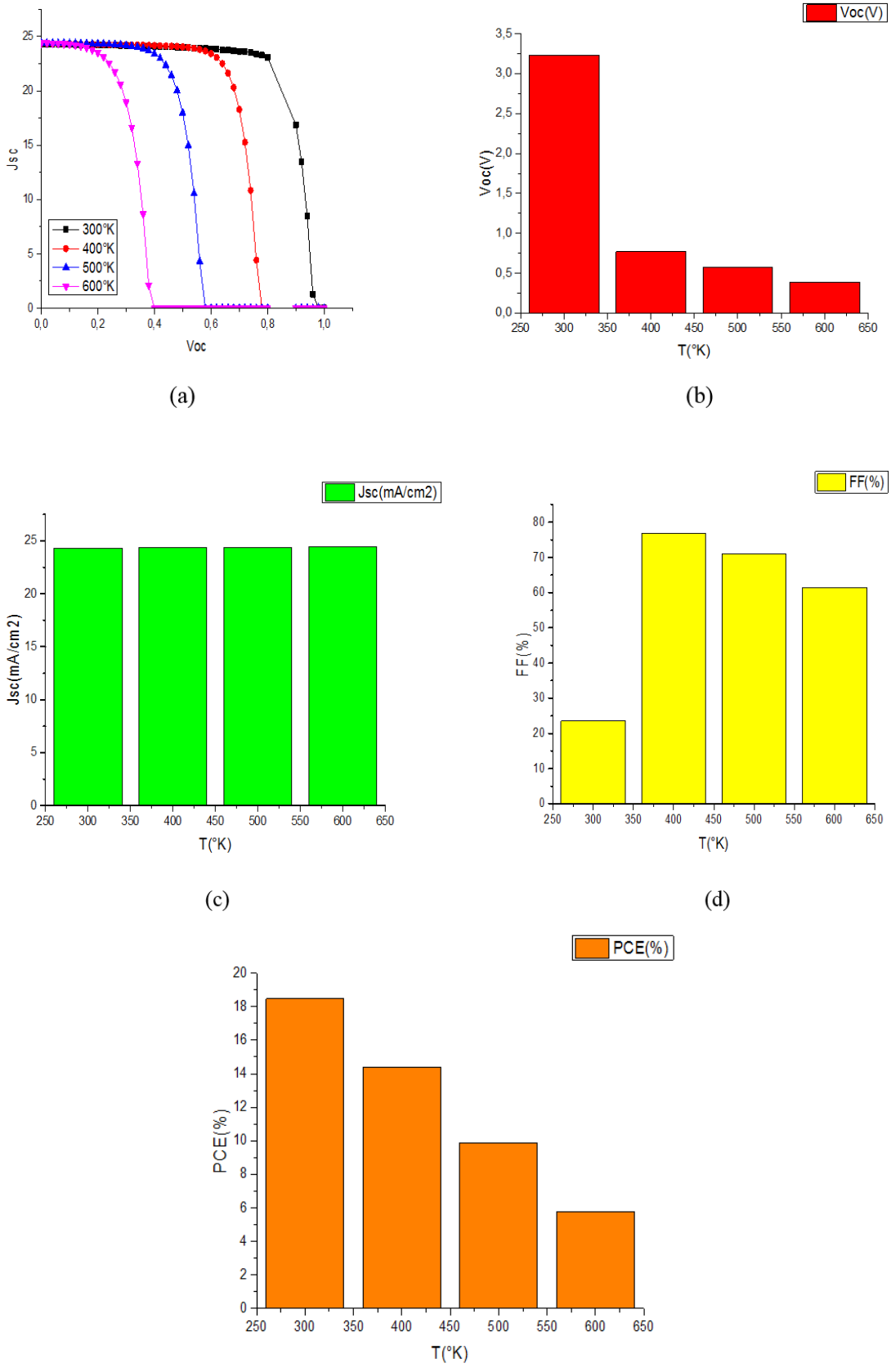

Figure 6. *Effect of temperature on J-V characteristics (a) and electrical parameters: (b)* V_{OC} *, (c)* J_{SC} *, (d)* FF *, and (e)* PCE *.*

4. Conclusion

In this work, we designed a solar device under the normal n-i-p configuration of *Glass / FTO / SnO_2 / IDL_1 / $CsGeI_3$ / IDL_2 / Cu_2O / Au*. Using SCAPS 1D software, weeValuated the impact of interface defect layers on our cell's performance. The study revealed that the thickness of the IDL_1 interface layer has a significant impact on the conversion efficiency of the device, as it promotes better electron transfer. Conversely, the electron affinity affects the cell's conversion efficiency more when the IDL_2 layer takes an energy value of 4.17eV. The injection of defects into or within the IDL_1 or IDL_2 layer reduces the performance of the device. Increasing the defect density hampers the efficiency of carrier flow. It increases the probability of recombination of electron-hole pairs, especially in the IDL_2 layer. As the temperature increases, the study showed that the performance of the solar device decreases. This leads to an increase in internal defects and degradation, resulting in an increase in recombination in the cell.

Abbreviations

IDL	Defect Interface Layers
HTL	Hole Transport Layer
ETL	Electron Transport Layer

Author Contributions

Alioune Sow: Conceptualization, Formal Analysis, Methodology, Writing – original draft, Writing – review & editing

Saliou Seck: Methodology

Modou Faye: Supervision, Visualization

Mamadou Salif Mane: Supervision, Validation

Amadou Ndiaye: Investigation, Methodology

Conflicts of Interest

The authors declare no conflicts of interest.

References

[1] Alioune SOW, Saliou Seck, Mamadou Salif Mane, Amadou Ndiaye, Bachirou Ndiaye, El-Hadji Mamadou Keita, Babacar Mbow, and Cheikh Sene. Effects of Transport Window Layers on All-inorganic $CsPbI_{3-x}Br_x$ Perovskites Based Solar Cells. American Journal of Energy Research, 2023, Vol. 11, No. 2, 93-99.

[2] S. SECK, A. Sow, M. S. Mané, A. Ndiaye, E. M. Keita, B. Ndiaye, B. Mbow, and C. Sène. Modeling and Analysis of a Mixed Sn-Ge Lead Free Perovskite Based Solar Cells. American Journal of Energy Research, 2024, Vol. 12, No. 1, 1-7.

[3] Xiangrui Menga, Tianhang Tanga, Ruitao Zhangb, Kaiyuan Liua, Wenhao Lia, Lan Yanga, Yubao Songc, Xinxia Maa, Zhihai Chenga, and Jiang Wu. Optimization of germanium-based perovskite solar cells by SCAPS simulation. Optical Materials, 128(2022), 112427.

[4] Xiaohui Li, Jianyao Tang, Putao Zhang, and Shengjun Li. Strategies for achieving high efficiency and stability in carbon-based all-inorganic perovskite solar cells. Cell Reports Physical Science 5, 2024, 101842.

[5] Junhua Lu, Shuo Chen, Hairong Wang, Long Qiu, Chenyu Wu, Wencan Qian, Zhijie Wang, Kai Huang, Jiang Wu, Huan Chen, and Yuxing Gao. Replacing the electron-hole transport layer with Doping: SCAPS simulation of lead-free germanium-based perovskite solar cells based on $CsGeI_3$. preprint research paper has not been peer reviewed. Electronic copy available at: https://ssrn.com/abstract=4625126

[6] M. Khalid Hossain, Mustafa K. A. Mohammed, M. Shihab Uddin, G. F. Ishraque Toki, Rahul Pandey, Md. Ferdous Rahman, D. P. Samajdar, Md. Rasidul Islam, JayaMadan, Sagar Bhattarai, H. Bencherif, Mongi Amamik and D. K. Dwivedil. Achieving above 24% efficiency with non-toxic $CsSnI_3$ perovskite solar cells by harnessing the potential of the absorber and charge transport layers. RSC Adv., 2023, 13, 23514–23537.

[7] Nurul Afiqah Buruhanutheen, Ahmad Sharmi Abdullah, Mohd Halim Irwan Ibrahim, Fauzan Ahmad and Mohd Haniff Ibrahim. Modeling of Germanium-Based Perovskite Solar Cell for Different Hole Transport Materials and Defect Density. PHOTONICS LETTERS OF POLAND, 2023, VOL. 15(3), 45-47.

[8] Deepthi Jayan Ka, Varkey Sebastiana, and Joji Kurian. Simulation and optimization studies on $CsPbI_3$ based inorganic perovskite solar cells. SolarEnergy, 2021, Vol 221, 99–108.

[9] T. Jesper Jacobsson, WolfgangTress, Juan-Pablo Correa-Baena, Tomas Edvinsson, and Anders Hagfeldt. Room Temperature a sa Goldilocks Environment for $CH_3NH_3PbI_3$ Perovskite Solar Cells: The Importance of Temperature on Device Performance. The Journal of Physical Chemistry, https://doi.org/10.1021/acs.jpcc.6b02858

[10] Lipsa Rani Karna, Rohitash Upadhyay, and Avijit Ghosh. All-inorganic perovskite photovoltaics for power conversion efficiency of 31%. Scientific Reports, (2023) 13: 15 212. https://doi.org/10.1038/s41598-023-42447-w

[11] Abhijeet J. Kale, Rajneesh Chaurasiya, and Ambesh Dixit. Inorganic Lead-Free $Cu_2AuBiCL_6$ Perovskite Absorber and Cu_2O Hole Transport Material Based Single-Junction Solar Cells with 22.18% Power Conversion Efficiency. Adv. Theory Simul. 2021, Vol 4, No 2000224, 1 of 14.

[12] Isabel Mesquita, Luísa Andrade, and Adélio Mendes. Temperature Impact on Perovskite Solar Cells Under Operation. ChemSusChem, https://doi.org/10.1002/cssc.201802899

[13] Thirumal Krishnamoorthy, Hong Ding, Chen Yan, Wei Lin Leong, Tom Baikie, Ziyi Zhang, Matthew Sherburne, Shuzhou Li, Mark Asta, Nripan Mathews, and Subodh G. Mhaisalkar. Lead-free Germanium Iodide Perovskite Materials for Photovoltaic Application. J. Name., 2013, 00, 1-3.

[14] Zhizai Li, Faguang Zhou, Qian Wang, Liming Ding b, and Zhiwen Jin. Approaches for thermodynamically stabilized CsPbI3 solar cells. Nano Energy, 2020, Vol 71, 104634.

[15] Tian Luo, Yufan Xia, Jiawei Huang, Xi Huang, Zhenyuan Wu, Yuxuan Chen, Xin Xu, Weiguang Xie, Pengyi Liu, Cuiying Hu, Xing Lu and Tingting Shi. Different structuraleVolutions of inorganic perovskite $CsGeI_3$. CrystEngComm, 2021, Vol 23, 4917.

[16] Shambhavi Rai, B. K. Pandey, and D. K. Dwivedi. Modeling of highly efficient and low cost $CH_3NH_3Pb(I_{1-x}Cl_x)_3$ based perovskite solar cell by numerical simulation. Optical Materials, 2020, Vol 100, 109631.

[17] Carlos Pinzón, Nahuel Martínez, Guillermo Casas, Fernando C. Alvira, Nicole Denon, Gastón Brusasco, Hugo Medina Chanduví, Arles V. Gil Rebaza and Marcelo A. Cappelletti. Optimization of Inverted All-Inorganic $CsPbI_3$ and $CsPbI_2Br$ Perovskite Solar Cells by SCAPS-1D Simulation. Solar 2022, 2, 559–571.

[18] Lingyan Lin, Linqin Jiang, Ping Li, Hao Xiong, Zhenjing Kang, Baodian Fan, Yu Qiu. Simulated development and optimized performance of $CsPbI_3$ based all-inorganic perovskite solar cells. Solar Energy, 2020, Vol 198, 454-460.

[19] Nahuel Martínez, Carlos Pinzón, Guillermo Casas, Fernando Alvira, Marcelo Cappelletti. Computational study of inverted all-inorganic perovskite solar cells based on $CsPbI_xBr_{3-x}$ absorber layer with band gap of 1.78eV. Accelerating the world's research, 2020.

[20] Xin Wu, Yizhe Liu, Feng Qi, Francis Lin, Huiting Fu, Kui Jiang, Shengfan Wu, Leyu Bi, Deng Wang, Fang Xu, Alex K.-Y. Jen and Zonglong Zhu. Improved stability and efficiency of perovskite/ organic tandem solar cells with an all-inorganic perovskite layer. Journal of Materials Chemistry A, 2021.

[21] Les Echos " Les émissions mondiales de CO_2 liées aux énergies fossiles vont battre un nouveau record cette année". Available from: https://www.lesechos.fr/monde/enjeux-internationaux/les-emissions-mondiales-de-co2-liees-aux-energies-fossiles-vont-battre-un-nouveau-record-cette-annee-2131160 [Accessed 14 December 2025].

[22] Bingcheng Yu, Chuantian Zuo, Jiangjian Shi, Qingbo Meng, and Liming Ding, ''Defect engineering on all-inorganic perovskite solar cells for high efficiency'', Journal of Semiconductors, 2021, Vol 42, 050203.